Xenopus Nonmuscle Myosin Heavy Chain Isoforms Have Different Subcellular Localizations and Enzymatic Activities

Christine A. Kelley,* James R. Sellers,* David L. Gard,§ Diane Bui,* Robert S. Adelstein,* and Ivan C. Baines‡

*Laboratory of Molecular Cardiology and ‡Laboratory of Cell Biology, National Heart, Lung, and Blood Institute, National Institutes of Health, Bethesda, Maryland 20892; and §The University of Utah, Department of Biology, Salt Lake City, Utah 84112

Abstract. There are two isoforms of the vertebrate nonmuscle myosin heavy chain, MHC-A and MHC-B, that are encoded by two separate genes. We compared the enzymatic activities as well as the subcellular localizations of these isoforms in *Xenopus* cells. MHC-A and MHC-B were purified from cells by immunoprecipitation with isoform-specific peptide antibodies followed by elution with their cognate peptides. Using an in vitro motility assay, we found that the velocity of movement of actin filaments by MHC-A was 3.3-fold faster than that by MHC-B. Likewise, the V_{max} of the actin-activated Mg^{2+}-ATPase activity of MHC-A was 2.6-fold greater than that of MHC-B. Immunofluorescence microscopy demonstrated distinct localizations for MHC-A and MHC-B. In interphase cells, MHC-B was present in the cell cortex and diffusely arranged in the cytoplasm. In highly polarized, rapidly migrating interphase cells, the lamellipodium was dramatically enriched for MHC-B suggesting a possible involvement of MHC-B based contractions in leading edge extension and/or retraction. In contrast, MHC-A was absent from the cell periphery and was arranged in a fibrillar staining pattern in the cytoplasm. The two myosin heavy chain isoforms also had distinct localizations throughout mitosis. During prophase, the MHC-B redistributed to the nuclear membrane, and then resumed its interphase localization by metaphase. MHC-A, while diffuse within the cytoplasm at all stages of mitosis, also localized to the mitotic spindle in two different cultured cell lines as well as in *Xenopus* blastomeres. During telophase both isoforms colocalized to the contractile ring. The different subcellular localizations of MHC-A and MHC-B, together with the data demonstrating that these myosins have markedly different enzymatic activities, strongly suggests that they have different functions.

MYOSIN is a diverse superfamily of molecular motors that is currently represented by 12 distinct classes based on sequence homology (40). Myosins of class II (Myosin II) have both a structural and an enzymatic role in such diverse cellular processes as muscle contraction (15), cell division (11), cell locomotion (47, 7), and intracellular movements (11, 25, 30). All myosin II proteins share the same basic molecular structure of a dimer of heavy chains of ~200 kD noncovalently associated with two pairs of light chains of 17 kD and 20 kD. The myosin heavy chain dimers form two globular amino-terminal heads and α-helical coiled-coil rods. The heads contain an actin-activated ATPase activity while the rods are involved in filament formation. Both the heavy chain and light chain subunits of myosin exist as isoforms. In this paper, we report our studies on the function of isoforms of the heavy chain of nonmuscle myosin II.

Please address all correspondence to C.A. Kelley, Laboratory of Molecular Cardiology, National Institutes of Health, Building 10, Room 8N-202, Bethesda, MD 20892. Tel.: (301) 496-5639. Fax: (301) 402-1542. E-mail: kelleyc@gwgate.nhlbi.nih.gov

There are at least two vertebrate nonmuscle myosin heavy chain (MHC)[1] genes (17, 18) that encode separate isoforms of the heavy chain, MHC-A and MHC-B. These isoforms are 87% identical at the amino acid level in the head region of the molecule and only 72% identical in the rod (45). Furthermore, there is greater sequence homology within the same isoform across species than between isoforms in the same species (45). In addition to significant differences in the primary sequence of MHC-A and MHC-B, the mRNAs encoding these isoforms are expressed in a tissue-dependent manner. In chickens, most tissues express different ratios of MHC-A and MHC-B mRNAs, with the extremes being spleen and intestinal epithelium which express almost exclusively the MHC-A isoform, and brain tissue which is enriched in MHC-B (18). Moreover, within a given tissue, different cell types may express different nonmuscle MHC II isoforms (29). Species differences in the relative expression of MHC-A and MHC-B

1. *Abbreviations used in this paper*: MOPS, 4-morpholinepropanesulfonic acid; MHC-A, nonmuscle myosin heavy chain A isoform; MHC-B, nonmuscle myosin heavy chain B isoform.

also exists as illustrated by *Xenopus* which, in contrast to avians, expresses mostly MHC-A and a small amount of MHC-B in all tissues examined (Kelley, C.A., unpublished observations). It is also interesting to note that in invertebrates, such as *Dictyostelium*, *Acanthamoeba*, *Drosophila*, and yeast, only one nonmuscle MHC isoform has been found (39). The expression of two different MHC isoforms in vertebrate nonmuscle cells is thus a recent evolutionary event raising the question as to whether MHC-A and MHC-B serve distinct functions.

Myosin function in nonmuscle cells was previously addressed in several studies by examining its subcellular distribution. Fujiwara and Pollard (9) identified myosin in cytoplasmic stress fibers as well as in the cleavage furrow and mitotic spindle of HeLa cells. However, the mitotic apparatus was stained much less intensely than the cleavage furrow, raising questions as to whether myosin was really concentrated in the mitotic apparatus. In contrast, Aubin et al. (1) found no myosin in the spindle but did find myosin in the cleavage furrow of PtK2 cells. Subsequently, Sanger et al. (38) injected fluorescent analogues of the myosin light chains into PtK2 cells to follow changes in the myosin distribution throughout the cell cycle. In interphase cells, myosin colocalized with stress fibers, while during mitosis a diffuse staining pattern in the spindle was observed. So, while there is little doubt as to the general distribution of nonmuscle myosin in interphase cells, it remains unclear as to the possible involvement of myosin in the mitotic spindle.

More recent studies have reported on the specific localization of the nonmuscle myosin heavy chain isoforms, MHC-A and MHC-B, within cells. Antibodies to brain myosin II (27) and MHC-B (5) stained the motile leading edge of growth cones in primary cultures of rat dorsal root ganglion cells. MHC-B colocalized with F-actin at the leading edge of growth cones as well as in the periphery of nonneuronal cells in the same dorsal root ganglion cultures. In contrast, MHC-A was confined to the perinuclear region of neuronal cell bodies which also showed a diffuse staining of MHC-B and actin. Antibodies to MHC-A also stained stress fibers in nonneuronal cells. Cheng et al. (5), the authors of the MHC-B study, speculated that MHC-B is probably involved in leading edge extension. However, a more recent study on the localization of MHC-A and MHC-B in cultured neurons suggests a role of MHC-B in retraction, not protrusion, of the growth cone periphery (35). Maupin et al. (26) examined two different tumor cell lines and found both MHC-A and MHC-B in small spots along stress fibers in interphase cells and a low concentration of diffuse MHC-B in the cortex of lamellipodia where MHC-A was not observed. MHC-A and B also colocalized in small spots in the cortex and in the cleavage furrow during mitosis, but no staining of the mitotic spindle was observed.

In addition to the generation of nonmuscle myosin heavy chain isoforms by different genes, the MHC-B pre-mRNA can be alternatively spliced to generate MHC-B isoforms with insertions and/or deletions of cassettes of amino acids near the ATP-binding region or the actin-binding region (45). We previously showed that in *Xenopus*, the majority (>90%) of the nonmuscle myosin in all cells is MHC-A, although a small amount of MHC-B, which constitutively contains the insert near the ATP-binding region, is also expressed (22; Kelley, C.A., unpublished results). This MHC-B isoform, but not the MHC-A isoform, was found to be serine-phosphorylated within the insert by $p34^{cdc2}$ kinase during meiosis in *Xenopus* oocytes (22). While the exact function of this phosphorylation is not known, these results demonstrated the potential for differential regulation of MHC-A and MHC-B and suggested that they may have different functions.

To further explore the possibility that MHC-A and MHC-B function differently in cells, we have purified and biochemically characterized these isoforms in vitro and we have found significant differences in enzymatic activity. We have also performed fluorescence immunolabeling studies using isoform-specific antibodies to precisely locate the myosin isoforms in interphase and mitotic cells. Our results demonstrate that these myosin isoforms have distinct distributions in both interphase and mitotic *Xenopus* A6 and XTC cells as well as in blastula-stage embryos, including the unique localization of MHC-A in mitotic spindles.

Materials and Methods

Tissue Culture

Xenopus A6 and XTC cells were grown at 25°C in Leibovitz L-15 medium diluted to 61% with water and supplemented with 10% FBS as described previously (43).

Antibody Production and Affinity Purification

Polyclonal rabbit antibodies specific for MHC-A and MHC-B were generated against synthetic peptides corresponding to unique amino acid sequences in the nonmuscle MHC isoforms. One MHC-B antibody (MHC-B (C)) was generated against the sequence SSSRSGRRQLHI which corresponds to an amino acid sequence near the carboxyl terminus of the chicken MHC-B sequence beginning at amino acid 1937. The *Xenopus* sequence differs by only one amino acid: the H is replaced by a Q. Another MHC-B antibody (MHC-B (I)) was raised against the sequence TESPKAIKHQSGLLY which corresponds to an inserted sequence near the ATP-binding region in the *Xenopus* MHC beginning at amino acid 212. Both of these antibodies were characterized previously (22).

Three different MHC-A antibodies were used. One was generated against the peptide sequence GKAEAGDAKATE corresponding to the carboxyl-terminal 12 amino acids of chicken MHC-A as described previously (45). A second MHC-A antibody was made against the peptide sequence DLDGKADSGDSKFVD, which was obtained from a partially cloned and sequenced *Xenopus* MHC-A (Conti, M.A., unpublished results) and corresponds to the carboxyl-terminal 15 amino acids of the heavy chain (MHC-A (C)). The third MHC-A antibody used was generated against human platelet myosin (19).

Conjugation of the peptides to keyhole limpet hemocyanin, immunization of rabbits, and affinity purification of the antisera were performed as described previously (20).

Myosin Purification

MHC-A and MHC-B were purified from 20 flasks (T175cm^2) of confluent *Xenopus* A6 cells. The cells were scraped from each flask with 0.20 ml of an extraction buffer containing 20 mM MOPS, pH 7.4, 60 mM KCl, 4 mM EDTA, 1 mM DTT, 10 mM $MgCl_2$, 5 mM ATP, 1.0% NP-40, 0.1 mM phenylmethane sulfonylfluoride (Sigma Chem. Co., St. Louis, MO), and 50 μg/ml leupeptin (Boehringer Mannheim Corp., Indianapolis, IN). The cell lysates were incubated on ice for 1 h followed by centrifugation at 100,000 *g* for 5 min at 4°C. The supernatants were recovered and incubated with the carboxyl-terminal MHC-B antibody overnight at 4°C. Pansorbin (Calbiochem-Novabiochem Corp., La Jolla, CA) was added to the immunoprecipitates for 2 h and the Pansorbin-antibody-MHC-B complexes were pel-

leted by centrifugation at 7,000 *g* for 5 min. The supernatants were removed for purification of MHC-A as described in the following paragraph. Each pellet was resuspended in 0.50 ml of extraction buffer and washed four times in a buffer containing 0.5 M NaCl, 50 mM MOPS, pH 7.4, and 0.1 mM EGTA to remove nonspecifically bound proteins. After the last wash, the pellets were resuspended in 0.2 ml of wash buffer containing a 50-fold molar excess of the peptide used to generate the MHC-B antibody. After 2 h the samples were centrifuged at 14,000 *g* for 5 min. The pellets contained Pansorbin bound to peptide-complexed antibody and the supernatants contained the released MHC-B and excess peptide. The MHC-B was concentrated and the peptide removed by repeated washing in a Centricon 100 (Amicon, Beverly, MA) or by dialysis against Aquacide (Calbiochem), to reduce the volume, followed by dialysis against several changes of wash buffer described above.

The supernatant generated following the pelleting of the Pansorbin-antibody-MHC-B complex was incubated overnight at 4°C with the carboxyl-terminal *Xenopus* MHC-A antibody. MHC-A was purified exactly as described above for MHC-B except that the peptide used to elute the MHC-A from the antibody corresponded to the carboxyl-terminal 15–amino acid sequence of MHC-A.

Gel Electrophoresis and Immunoblotting

Gel electrophoresis was performed in SDS-5% polyacrylamide and 0.065% bisacrylamide or SDS-12.5% or 8-16% polyacrylamide with 0.13% bisacrylamide using the buffer system of Laemmli (23). The proteins in the gels were either stained with Coomassie Brilliant blue or electrophoretically transferred to Immobilon-P (Millipore, Bedford, MA) and immunostained with affinity-purified antibodies as described (20).

Assays for Myosin Activity

The sliding actin filament assay was performed and analyzed as described previously (20) with two modifications: (*1*) myosin was introduced into the assay as monomers in a buffer containing 0.5 M NaCl, 50 mM MOPS, pH 7.4, and 0.1 mM EGTA and (*2*) the motility buffer contained 80 mM KCl, 20 mM MOPS, pH 7.2, 5 mM $MgCl_2$, 0.1 mM EGTA, 1 mM ATP, 50 mM DTT, 0.2 μM tropomyosin, 2.5 mg/ml glucose, 0.1 mg/ml glucose oxidase, and 0.02 mg/ml catalase.

Actin-activated Mg^{+2}-ATPase activities were assayed in a final volume of 0.1 ml containing 0.05–0.10 mg/ml myosin, 50 mM KCl, 10 mM $MgCl_2$, 20 mM MOPS, pH 7.0, 0.2 mM EGTA, 1 mM [γ-^{32}P]ATP, 2 mM DTT in the absence or presence of various concentrations of F-actin from 0.5 to 45 μM at 37°C. Aliquots were removed at various times and P_i release was measured as described by Pollard and Korn (33). The maximum ATPase activity (Vmax) and the actin concentration at ½ V_{max} (K_{ATPase}) were determined by fitting the data to the Michaelis-Menton equation.

Confocal Immunofluorescence Microscopy

Xenopus A6 and XTC cells were cultured on glass coverslips in growth medium as described above and were processed for indirect immunofluorescence by either of two methods (2). Briefly, method 1 involved simultaneous fixation and permeabilization by immersion of cells in 1% formalin in methanol at −20°C for 10 min, followed by air drying, rehydration in PBS, and treatment of the cells with 100 mM NH_4Cl for 20 min (to reduce background fluorescence due to formalin). For method 2, cells were fixed in 3.7% formalin in growth medium for 20 min, fixed for an additional 20 min in 3.7% formalin in PBS, permeabilized in 100% acetone for 30 s at −20°C, air dried, rehydrated in PBS, and treated with 100 mM NH_4Cl as before. In some experiments, the second method was modified to include 0.1% glutaraldehyde in the fixative (3.7% formalin, 0.1% glutaraldehyde) and/or cells were permeabilized with a 10-min incubation in 0.2% TX-100 in PBS instead of acetone. When glutaraldehyde was included in the fixative, free aldehydes were reduced after fixation (and washing of the cells in PBS) by two incubations in 1 mg/ml sodium borohydride, for 10 min each. In all experiments, after fixation, nonspecific binding of antibodies was blocked by incubation in blocking buffer (1% BSA, 50 mM L-lysine, 0.01% thimerosal in PBS, pH 7.4) for 30 min. Cells were incubated in primary antibodies diluted either 1:20 (all antibodies to myosin) or 1:50 (anti-tubulin; Amersham Life Sciences, UK) and in fluorophore-conjugated secondary antibodies (Molecular Probes, Eugene, OR) at a concentration of 15 μg/ml. All antibodies were diluted in blocking buffer, incubations were for 1.5 h at 37°C, and cells were washed five times for 5 min each in PBS between incubations and after the secondary antibody incubation. In double-labeling experiments, cells were incubated in anti-tubulin antibodies either before, simultaneously, or after myosin antibodies (all permutations were tested and did not influence the staining patterns). F-actin was detected with rhodamine phalloidin (Molecular Probes) after the second antibody incubation, according to the manufacturers' protocol. In filament disruption experiments, F-actin was depolymerized by exposure of the cells to 15 μg/ml cytochalasin B for 30 min or microtubules were depolymerized by treatment of cells with 30 μg/ml nocodazole for 1 h (cytochalasin B and nocodazole were added to the cells in growth medium before fixation). After the final wash in PBS, cells were mounted in fluorescence mounting medium (Kirkegaard and Perry, Gaithersburg, MD) and were viewed on a Zeiss Axiovert 135 inverted microscope with a ×63 neofluor objective and a Zeiss LSM 410 confocal attachment. All micrographs were taken with identical contrast and brightness settings.

Confocal immunofluorescence microscopy of methanol or formalin-glutaraldehyde fixed 6–8 h *Xenopus* blastulae was performed as previously described (12) using antibodies to chicken or *Xenopus* MHC-A and MHC-B (MHC-B(I) and MHC-B(C)) and rhodamine-conjugated anti-rabbit IgG (Cappell, Malvern, PA). Affinity-purified antibodies were diluted1/25–1/200 in TBS containing 0.1% NP-40 and 1% BSA to reduce nonspecific background. Control embryos were incubated in the absence of primary, or in comparable dilutions of normal rabbit serum. Embryos were cleared in benzyl alcohol:benzylbenzoate (1:2) and mounted as described (12). Embryos were examined using a Nikon Optiphot with a Biorad MRC-600 laser-scanning confocal microscope. Optical section thicknesses were 1–2 μm.

Results

Purification of MHC-A and MHC-B from Xenopus A6 Cells

We used isoform-specific, affinity-purified antibodies to purify enzymatically active MHC-A and MHC-B from cultured *Xenopus* A6 cells. MHC-B was immunoprecipitated from a total cell extract and subsequently eluted from the antibody with the synthetic peptide used to generate the antiserum. The extract supernatant remaining after depletion of MHC-B was incubated with an MHC-A specific antibody, and, following immunoprecipitation, the MHC-A was similarly eluted from the antibody with the cognate peptide antigen. Isoform purity was analyzed by 12.5% and 5% SDS-PAGE and Coomassie-blue staining as well as by immunoblotting (Fig. 1). Fig. 1 *A*, lane *2* shows the protein profile of the A6 cell extract from which the myosin isoforms were purified. Purified MHC-A (Fig. 1 *A*, lane *3*) contains one major band at 200 kD, which is the predicted molecular weight of the myosin heavy chain. The 20- and 17-kD light chains are barely visible at this level of protein loading. In addition to MHC-A at 200 kD, a minor band is seen at ~50 kD that occasionally copurifies with MHC-A and MHC-B and comigrates with the affinity-purified IgG heavy chain (data not shown). The presence of this carboxyl-terminal antibody did not effect myosin enzyme activity (data not shown) and thus further purification was not required. Purified MHC-B appears to be completely free of other proteins (Fig. 1 *A*, lane *4*). *Xenopus* A6 cell extracts, separated to a greater extent in SDS-5% polyacrylamide gels, show one major band at 200 kD (Fig. 1 *B*, lane *2*). We previously identified this band as MHC-A (22). The amount of MHC-B in these cells is too low to be detected by Coomassie-blue staining of whole cell extracts. Purified MHC-A (Fig. 1 *B*, lane *3*) migrates as a single band with a slightly faster relative mobility than

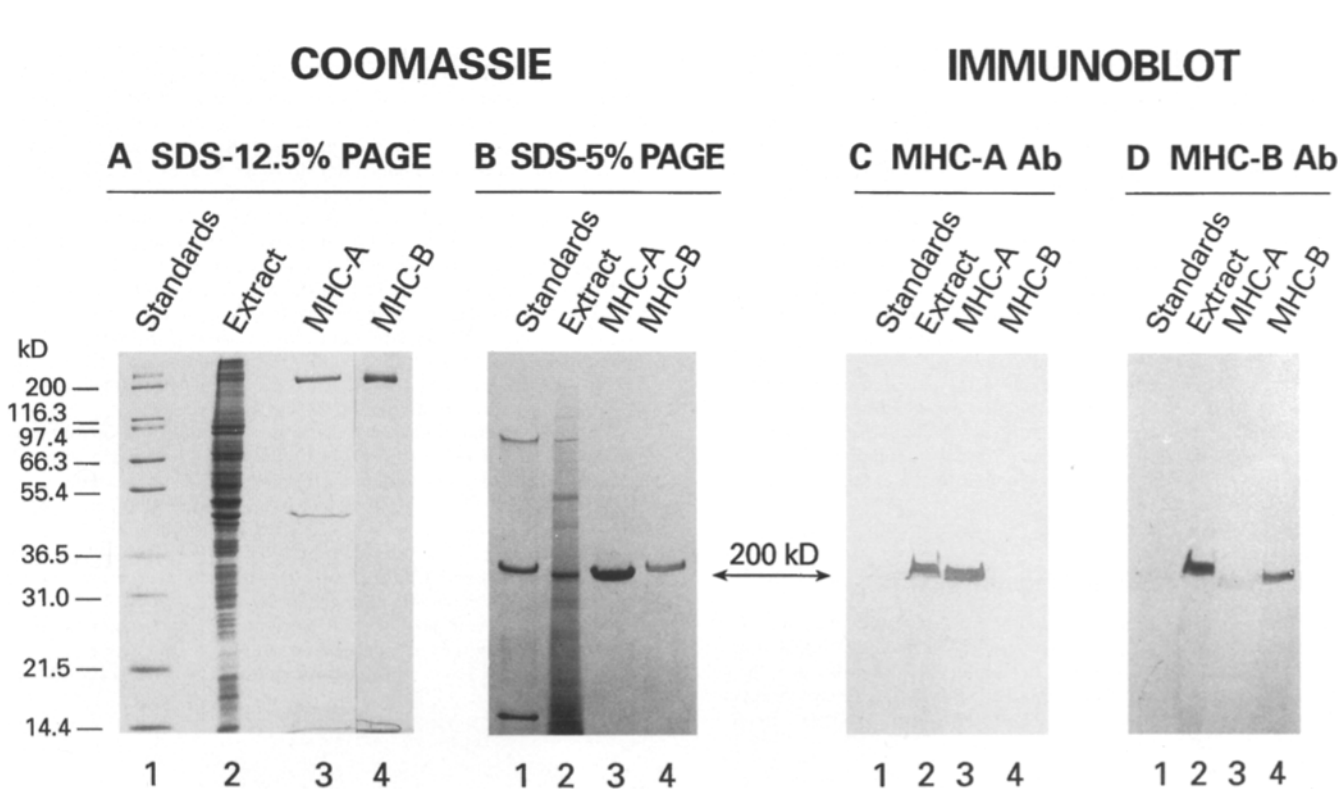

Figure 1. Analysis of purified MHC-A and MHC-B. (*A*) Coomassie-blue stained SDS-12.5% polyacrylamide gel of MHC-A and MHC-B purified by immunoprecipitation from A6 cell extracts, and then released from the antibodies with the peptide antigen as described in Materials and Methods. (Lane *1*) Molecular weight standards; lane *2*, whole A6 cell extract; lane *3*, purified MHC-A; lane *4*, purified MHC-B. (*B*) SDS-5% polyacrylamide gel analysis of purified MHC-A and MHC-B. Lanes *1–4* contain the same samples as those indicated for *A*, lanes *1–4*. Lane *3* shows one major band for MHC-A at ~200 kD while MHC-B (lane *4*) contains two bands. (*C* and *D*) Immunoblots of SDS-5% polyacrylamide gels. Lanes *1–4* contain the same samples as in *A*, lanes *1–4*. The proteins, which were transferred to Immobilon, were probed with either an antibody to the *Xenopus* MHC-A carboxyl-terminal peptide (MHC-A (C), *C*) or probed with the antibody to the *Xenopus* MHC-B inserted region (MHC-B (I), *D*).

that of purified MHC-B (Fig. 1 *B*, lane, *4*) which migrates as a doublet. Previously, we observed this doublet pattern in *Xenopus* XTC cells (22) and speculated that the two bands probably represent the products of duplicated genes, a common occurrence in *Xenopus*, and previously demonstrated for the MHC-B gene (4).

The purified myosins were further characterized by immunoblotting of proteins separated in SDS-5% polyacrylamide gels. Fig. 1 *C* shows the immunoreactivity of the proteins with an antibody to the carboxyl terminus of *Xenopus* MHC-A (MHC-A (C)). The antibody recognizes one band at ~200 kD in the whole cell extract (lane *2*) as well as the purified MHC-A (lane *3*). In contrast, the antibody does not recognize any molecular weight standards (lane *1*) or purified MHC-B (lane *4*). Fig. 1 *D* shows the immunoreactivity of the proteins to a MHC-B–specific insert antibody (MHC-B (I)). This antibody recognizes a 200-kD band in the whole cell extract (lane *2*) as well as in the purified MHC-B (lane *4*). Both bands of purified MHC-B detected by Coomassie-blue staining (Fig. 1 *B*, lane *4*) were recognized by immunoblotting, despite the poor resolution of these two bands after transfer (data not shown). It is particularly noteworthy that the MHC-A and MHC-B antibodies did not display any cross-reactivity, as demonstrated by Fig. 1 *C*, and *D* and that the purified MHC-A is completely free of MHC-B and the MHC-B is not contaminated with any MHC-A.

Comparison of Enzymatic Activities of MHC-A and MHC-B

We compared the velocity of movement of actin filaments by purified MHC-A and MHC-B using an in vitro sliding actin filament assay. Fig. 2 shows the velocity distributions for actin filaments being propelled by either MHC-A (*open bars*) or MHC-B (*hatched bars*). MHC-A moved actin filaments at an average velocity of 0.723±0.166 μm/s which was 3.3-fold faster than the velocity of movement of actin filaments by MHC-B (0.216±0.028 μm/s).

Purified MHC-A and MHC-B were further characterized by measuring actin-activated Mg^{2+}-ATPase activities (Table I). These activities were measured in the presence of various concentrations of F-actin from 0.5 to 45 μM. V_{max} and K_{ATPase} were determined from double-reciprocal plots. Similar to the results of the in vitro motility assay, the V_{max} of the actin-activated ATPase activity for MHC-A (0.746±0.28 s^{-1}) was 2.6-fold higher than that of MHC-B (0.290±0.058 s^{-1}). Both myosins showed similar affinities for actin (K_{ATPase} = 16.5 μM for MHC-A and 20.8 μM for MHC-B).

Subcellular Localization of MHC-A and MHC-B in Interphase Cells

For further clues of the specific functions of MHC-A and MHC-B, we examined the subcellular distributions of

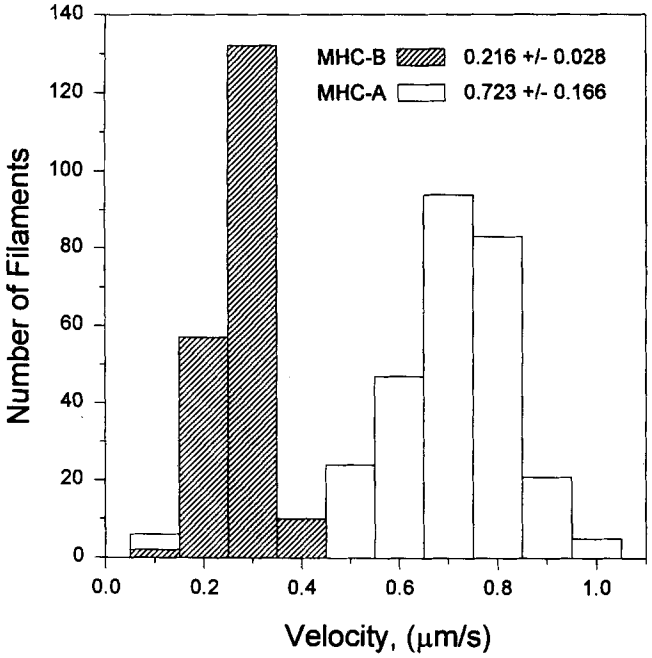

Figure 2. Translocation of actin filaments by MHC-A and MHC-B in a sliding filament motility assay. Histograms of the velocity distributions for actin filaments sliding over MHC-B (*hatched bars*) or MHC-A (*open bars*). The average velocities±the standard deviations are shown in the upper right corner and are expressed as μm/s. The results shown are from one experiment. However, similar results were obtained in at least four separate experiments using four different preparations of both MHC-A and MHC-B.

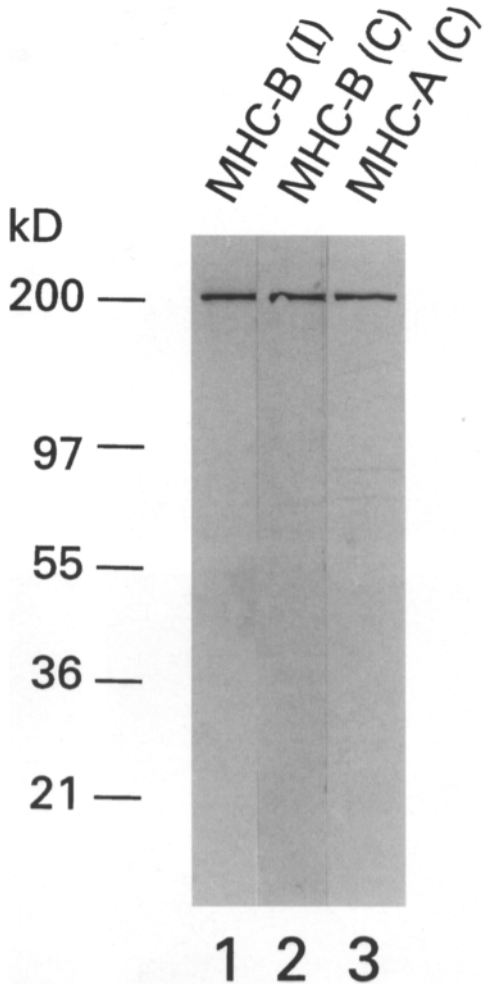

Figure 3. Characterization of the MHC-A and MHC-B antibodies used for immunolocalization. Immunoblots of A6 cell extracts electrophoresed in 8–16% polyacrylamide gradient gels. Lane *1*, immunoreactivity of the extract with the MHC-B insert antibody (MHC-B (I)); Lane *2*, extract probed with MHC-B carboxyl-terminal antibody (MHC-B (C)); Lane *3*, reactivity of the extract with the *Xenopus* MHC-A carboxyl-terminal antibody (MHC-A (C)).

these isoforms in cultured *Xenopus* cells. The antibodies used, MHC-B (C), MHC-B (I), and MHC-A (C), were described under Materials and Methods. In Fig. 1 we demonstrated the specificity of the antibodies for the MHC-A and MHC-B isoforms on low percentage polyacrylamide gels. For immunostaining, we first determined the specificity of the antibodies for myosin, compared to other cellular proteins, by immunoblotting cell extracts electrophoresed in SDS 8–16% acrylamide gradient gels. Fig. 3 shows that both of the MHC-B specific antibodies (MHC-B (I) and MHC-B (C)) and the MHC-A specific antibody react only with myosin. The specificity of the MHC-A and MHC-B antibodies allowed us to look at the subcellular distribution of these isoforms in cultured *Xenopus* A6 and XTC cells. In addition, we examined their localization in relation to microfilaments and microtubules by double-labeling the cells with either rhodamine phalloidin or antibodies to tubulin, respectively.

Fig. 4 *a* shows the colocalization of MHC-A with actin. Actin is present in the cell cortex as well as in stress fibers within the cytoplasm. MHC-A is notably absent from the cell cortex and is found to partially colocalize with stress fibers within the cytoplasm as well as have a fibrillar staining pattern apart from stress fibers. In contrast, as shown in Fig. 4 *b*, MHC-B colocalizes with F-actin in the cell periphery (*arrows*), a region in which MHC-A is absent, and displays a diffuse staining pattern within the cytoplasm, an area where MHC-A is present as filaments. Although the yellow fluorescence of the actin filaments in Fig. 4 *b* appears to indicate some colocalization of MHC-B with stress fibers, this is because the red stress fibers are imaged against a diffuse background of green MHC-B fluorescence. There is no actual colocalization, just coincident superimposition.

Table I. Kinetics of the Actin-activated Mg^{+2}-ATPase Activity of MHC-A and MHC-B

Parameter measured	Myosin isotype	
	MHC-A	MHC-B
V_{max} (s^{-1})	0.746 ± 0.28	0.290 ± 0.058
K_{ATPase} (μM)	16.5	20.8

The Mg^{+2}-ATPase activity of phosphorylated myosin in the absence of actin was subtracted from each data point. The results represent the average of three separate experiments performed with three different myosin preparations. The data were computer fitted to the Michaelis-Menton equation by nonlinear regression. The means plus or minus the standard deviations are shown.

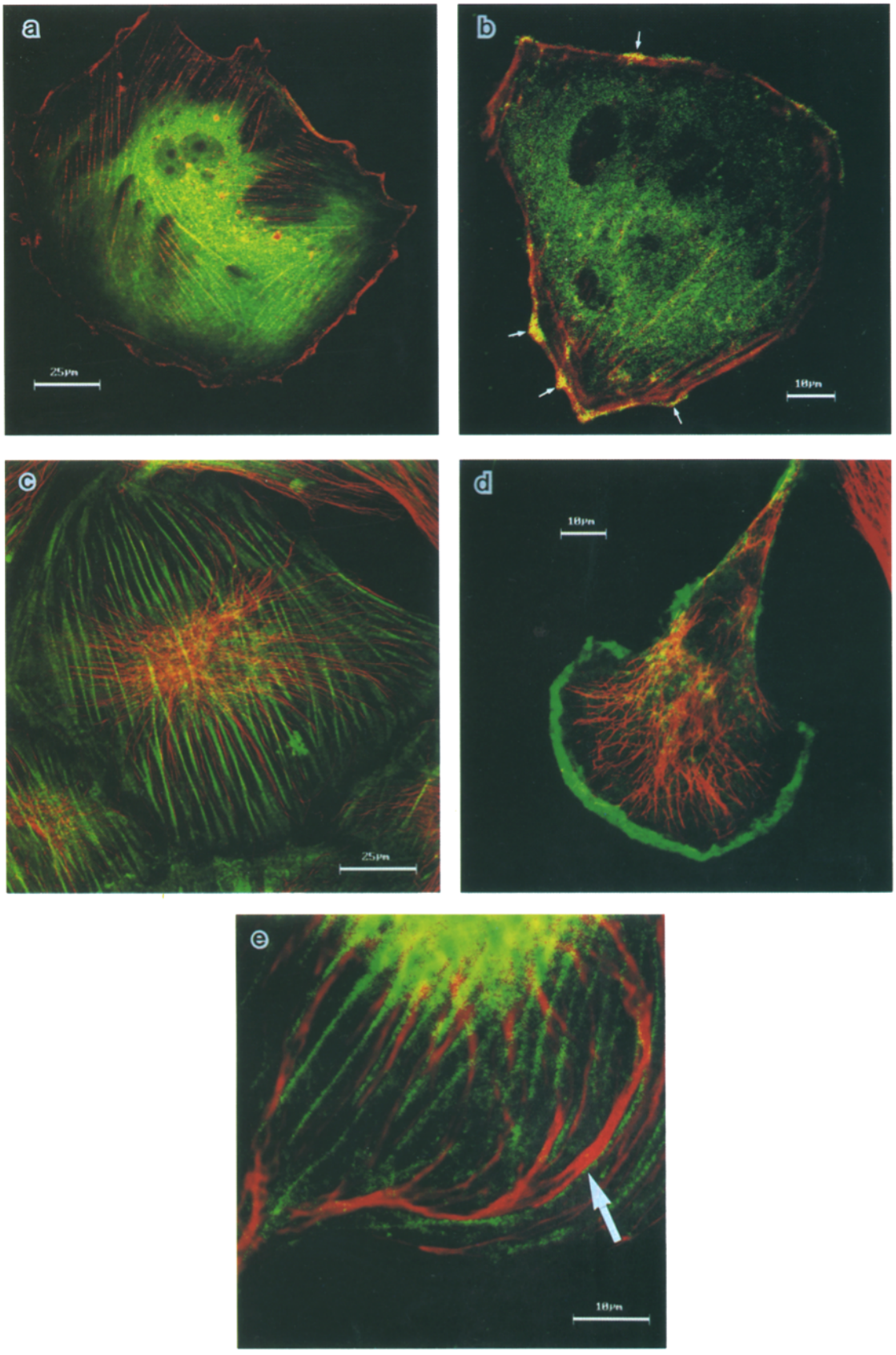

Figure 4. Immunofluorescence localization of MHC-A and MHC-B in cultured *Xenopus* A6 cells. Cells were fixed as described under Materials and Methods and prepared for indirect confocal immunofluorescence microscopy using the MHC-A(C) or MHC-B(I) affinity-purified antibodies. Cells were double labeled with either rhodamine phalloidin to stain F-actin or anti-tubulin antibodies to stain microtubules. Myosin staining is green, actin or tubulin staining is red, and the overlap is yellow. (*a*) Cells were fixed by method 2 and

Because the staining pattern for MHC-A did not correlate 100% with the stress fiber staining pattern, we looked to see if there was any component of the MHC-A staining that colocalized with microtubules. Fig. 4 *c* shows a *Xenopus* A6 cell double stained for MHC-A and microtubules. Some components of the MHC-A staining pattern are coincident with microtubules while others are not. The juxtaposition of microtubules and MHC-A is suggestive of an interaction between MHC-A and microtubules or F-actin and microtubules. This is particularly evident at higher magnification (*e*), where MHC-A and microtubules appear to be in contact (at the level of resolution of the fluorescence microscope which is ~0.2 μm) in certain regions (*arrow*) while in other regions they follow parallel but separate paths within 1 μm of each other. MHC-B (Fig. 4 *d*) also has a localization distinct from microtubules. The cell in *d* has adopted a highly polarized morphology which is characteristic of rapidly migrating cells. The broad lamellipodium at the front of the cell is dramatically enriched for MHC-B. This is particularly striking since the lamellipodium is the thinnest region of the cell (<2 μM). There is no diffuse cytoplasmic staining of MHC-B as was seen in the cell in Fig. 4 b. This suggests that one event in the polarization of these cells must be a change in MHC-B distribution from the cell cortex and cytoplasm to the leading edge resulting in the spatial asymmetry of MHC-B shown in Fig. 4 *d*. This localization reflects a possible involvement of MHC-B in the extension and/or retraction of protrusions in locomoting cells.

Effects of Microfilament and Microtubule Disruption on MHC-A and MHC-B Localization

To confirm the colocalization of MHC-A and MHC-B with microfilaments, but not microtubules, A6 cells were treated with either cytochalasin B to depolymerize F-actin, or nocodazole to disassemble the microtubule network, and then doubled stained for either MHC-A or MHC-B together with rhodamine phalloidin or anti-tubulin antibodies. When cells were treated with cytochalasin B, the microfilament system completely collapsed resulting in an increased concentration of G-actin in the cytoplasm, particularly surrounding the nucleus (data not shown), and the presence of highly localized foci of residual F-actin (detected by phalloidin) present throughout the cell but most abundant at the periphery of the cell (Fig. 5 *b*). The MHC-A filaments in cells also collapsed to the perinuclear region on cytochalasin B treatment while the microtubules were unperturbed (Fig. 5 *a*). These results demonstrate that MHC-A is associated with actin filaments and that depolymerization of F-actin leads to the collapse of the associated MHC-A filaments. Cytochalasin B also disrupted MHC-B localization but in a manner distinct from its effect on MHC-A. When A6 cells were treated with cytochalasin B, actin filaments were mostly depolymerized while the MHC-B collapsed with residual F-actin into spots that were localized primarily in the cell periphery (Fig. 5 *b*). This population of collapsed MHC-B probably represents that which localized in the cell periphery with actin in untreated cells (Fig. 4 *b*). The small amount of MHC-B seen in the center of the cell shown in Fig. 5, *b* and *c* most likely represents the diffuse, soluble MHC-B seen in untreated cells such as that shown in Fig. 4 *b*. The actin population which collapses to the nucleus together with MHC-A appears to be completely depolymerized and is therefore not detected by phalloidin. Fig. 5 *c* shows that the microtubules are intact in cells treated with cytochalasin B and the collapsed spots of MHC-B, which also contain F-actin (as shown in Fig. 5 *b*), are localized at the tips of microtubules.

When A6 cells are treated with nocodazole, the microtubules are depolymerized, but the actin cytoskeleton, as well as the MHC-A and MHC-B localizations, are undisturbed (data not shown). This is further evidence for the colocalization of MHC-A and MHC-B with microfilaments, but not microtubules, within the cell.

Subcellular Localization of MHC-A and MHC-B in Mitotic Cells

Fig. 6, *a–c*, summarizes the pattern of staining during various stages of mitosis in A6 cells that were double labeled for MHC-A or MHC-B (using the MHC-A(C) and MHC-B(I) antibodies) and microtubules. Fig. 6 *a* shows that MHC-A is diffuse in the cytoplasm and concentrated mainly at the spindle poles (*arrow*) in early prophase. In metaphase as shown in Fig. 6 *b*, anti–MHC-A staining, like that reported previously for total myosin (9, 38), is observed within the mitotic spindle as well as the cytoplasm. MHC-A fluorescence is punctate in the region of the spindle with particularly bright spots of fluorescence in close association with spindle microtubules (Fig. 6 *b*, *arrows*). Similar staining was seen using two additional MHC-A antibodies (see Materials and Methods) in cultured A6 and XTC cells. No spindle staining was ever seen in A6 or XTC cells, with either of the MHC-B specific antibodies (Fig. 6 *e*). By early telophase, the MHC-A staining was confined to the contractile ring as shown in Fig. 6 *c*.

stained for MHC-A and actin. Actin is present in the periphery of the cell as well as in stress fibers in the cytoplasm. MHC-A is notably absent from the periphery and is present as filaments, partially colocalizing with stress fibers, within the cytoplasm; (*b*) cells were fixed by method 2 and stained for MHC-B and actin. MHC-B colocalizes with F-actin in the cell periphery (*arrows*) and has a diffuse (soluble) staining pattern within the cytoplasm; (*c*) cells were fixed by method 1 and stained for MHC-A and tubulin. Some components of the MHC-A staining pattern are coincident with microtubules while others are not. MHC-A and microtubules are in close juxtaposition but do not colocalize; (*d*) cells were fixed by method 1 and stained for MHC-B and tubulin. MHC-B has a localization distinct from that of microtubules. This highly polarized cell has adopted a morphology characteristic of rapidly migrating cells. The broad lamellipodium at the front of the cell is dramatically enriched for MHC-B, particularly since the lamellipodium is the thinnest region of the cell (<2 μM). (*e*) high magnification image of a cell fixed by method 1 and stained for MHC-A and microtubules. At this magnification, MHC-A filaments can be seen to run in close apposition with microtubules, often appearing to be in actual contact for distances greater than 50 μM (see arrow). It is also evident that although the two filaments are closely apposed, they do not actually colocalize. Bars: (*a* and *c*) 25 μm; (*b*, *d*, and *e*) 10 μm.

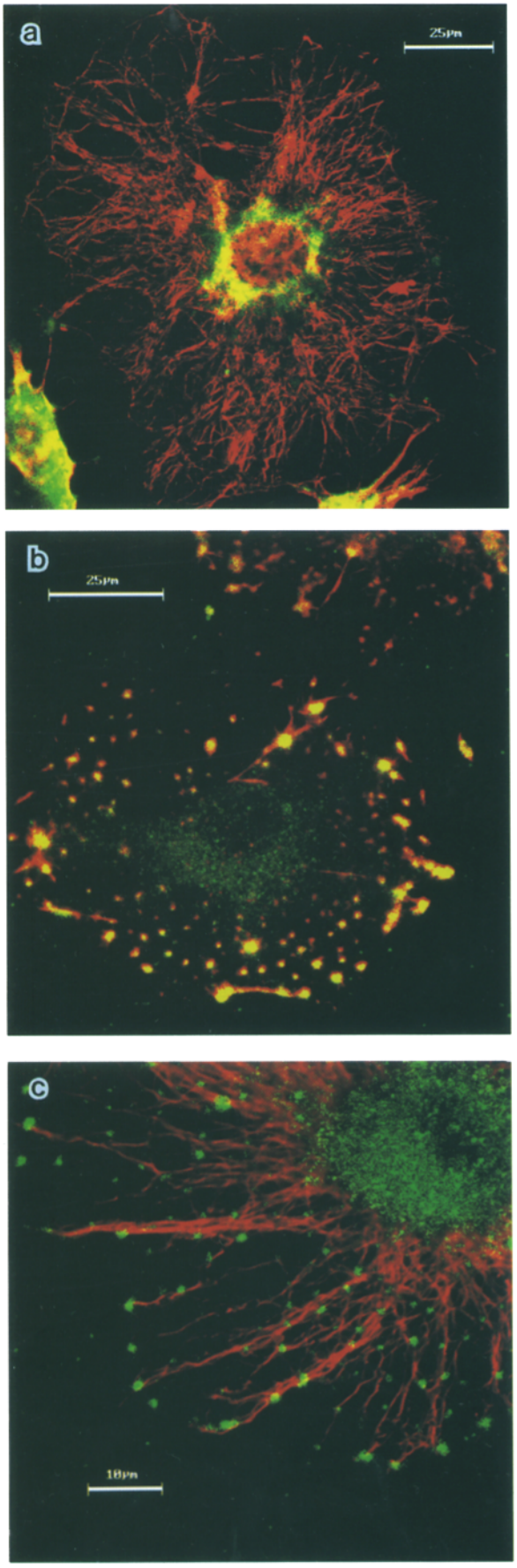

Fig. 6, *d–f* summarizes the sequence of MHC-B and microtubule rearrangements during mitosis. In the transition from interphase (Fig. 4 *b*) to prophase (Fig. 6 *d*), MHC-B moved from its cortical and diffuse cytoplasmic location to the nuclear envelope. The microtubules in this prophase cell (Fig. 6 *d*) are not yet assembled into the mitotic spindle. In the cell shown in Fig. 6 *e*, the spindle is fully assembled and the shadow of chromosomes can be seen midway between the spindle poles indicating that this cell is in metaphase. Interestingly, the MHC-B appears to have resumed its interphase localization. There is no indication of any spindle staining with the anti–MHC-B antibodies, in contrast to what was seen with our anti–MHC-A antibodies (compare Fig. 6, *b* and *e*). Fig. 6 *f* shows that in late telophase MHC-B, similar to MHC-A (Fig. 6 *c*), is found in the contractile ring.

Myosin Heavy Chain A Is Localized in the Mitotic Spindles of 6–8 h Xenopus Blastomeres

We also examined the subcellular distribution of myosin isoforms in 6–8 h *Xenopus* embryos. A consistent pattern was not observed in blastulae stained with either MHC-B antisera (results not shown). However, most cells exhibited a punctate cytoplasmic staining that was clearly distinct from that observed with normal rabbit serum. In contrast, affinity-purified MHC-A antibodies (Fig. 7) exhibited bright staining in both interphase (A) and mitotic (B) cells. MHC-A containing foci were clustered into two perinuclear aggregates, corresponding to the characteristic location of the centrosomes in these cells (13). In mitotic cells, a cloud of MHC-A containing foci was clustered around the mitotic spindle and astral microtubules. The spindle has a similar staining pattern to that observed for MHC-A in mitotic A6 cells (Fig. 6 *b*). However, the relative concentration of MHC-A in the mitotic spindle of blastomeres, compared with the rest of the cell, is much greater than was observed for A6 cells.

The punctate nature of the MHC-A staining suggested that the antibody might be staining a population of myosin-containing vesicles associated with both interphase microtubule arrays and mitotic spindles in early embryogenesis. To address this issue, we extracted blastula-stage embryos with microtubule stabilizing buffer containing 0.5% Triton X-100. As shown in Fig. 7, extraction for 75 min with detergents significantly reduced MHC-A staining associated with both interphase microtubules (*C*) and spindles (*D*), while tubulin staining remained largely unaffected (*E* and *F*).

Figure 5. Effect of cytochalasin-B on MHC-A and MHC-B localization in *Xenopus* A6 cells. After incubation in the presence of cytochalasin B, cells were fixed and permeabilized by method 2 and stained for MHC-A and tubulin (*a*); MHC-B and actin (*b*), and MHC-B and tubulin (*c*). Myosin staining is green, actin and tubulin staining are red, and the overlap of the fluorophores is yellow. MHC-A, along with actin (not shown), collapses to the nucleus in cytochalasin B–treated cells while the microtubules are unperturbed (*a*). MHC-B collapsed with residual F-actin into spots that were localized primarily in the cell periphery (*b*). The collapsed spots of MHC-B (and actin) are localized mainly at the tips of microtubules (*c*). Bars: (*a* and *b*) 25 μm; (*c*) 10 μm.

Discussion

Our results demonstrate that the two *Xenopus* nonmuscle MHC isoforms, MHC-A and MHC-B, differ functionally: MHC-A propels actin filaments at a markedly higher velocity, and exhibits a higher actin-activated ATPase activity than MHC-B. The different subcellular localizations of these isoforms during interphase and mitosis also suggest that they have unique functions. Moreover, their unique subcellular localizations in *Xenopus* cells suggests that these two isoforms do not form heteropolymers in vivo. Furthermore, immunoprecipitation experiments show that MHC-A and MHC-B can be obtained separately from whole cell extracts, and thus apparently do not form heterodimers to any significant extent.

In an effort to understand the molecular basis for the observed differences in enzyme activity and the homotypic association of these MHC isoforms, we looked for differences in the amino acid sequences between MHC-A and MHC-B that were conserved among species. We compared the sequences of MHC-A and MHC-B from *Xenopus* (Conti, M.A., and N. Bhatia-Dey, unpublished results; 4), chickens (45, 41), and humans (37, 42). Despite being the product of two separate genes, MHC-A and MHC-B are ~87% identical in the head region and ~72% identical in the rod. Interestingly, many of the non-identical residues are clustered. Although we cannot identify at this time exactly which of the clusters of divergent residues between MHC-A and MHC-B contribute to the different enzymatic activities and/or to the homotypic association of nonmuscle myosin dimers and filaments seen in *Xenopus* cells, we can point to regions of potential functional significance. Of particular interest are the two disordered loops, Loop 1 and Loop 2, which, because of their flexibility, were not resolved in the myosin crystal structure (34). Our comparison of the primary sequences of MHC-A and MHC-B showed that these regions are divergent in both length and amino acid sequence. Loop 1 is near the ATP-binding pocket, and Loop 2 is at the actin-binding region. Structural studies indicate that Loop 2 interacts with the negatively charged amino-terminal part of actin. Spudich (44) and Uyeda et. al (46) proposed that this loop is involved in tuning the critical rate constant that determines the V_{max} of the actin-activated ATPase although recent data by Rovner et al. (36) does not support this hypothesis. The function of Loop 1 remains to be determined. However, because of its proximity to the ATP-binding pocket it is likely to affect myosin enzyme kinetics. Previously, we found that an insert in Loop 1 of the smooth muscle MHC, in the exact same region of the molecule as the insert in nonmuscle MHC-B, results in a myosin with higher enzymatic activity than a non-inserted myosin (21). The differences in motility and ATPase between MHC-A and MHC-B reported here could also be due to the insert of 16 amino acids near the ATP-binding region in MHC-B. All of the MHC-B expressed in *Xenopus* contains this insert and therefore it was not possible to compare non-inserted MHC-B and MHC-A. However, it has been reported that the non-inserted heavy meromyosin fragment of chicken nonmuscle MHC-B expressed in the baculovirus expression system shows no significant difference in either motility or actin-activated $Mg^{+}2$-ATPase activity from the inserted (in this case 10 amino acids vs 16 in *Xenopus*) isoform (31). Therefore, it is possible that we are looking at differences between MHC-A and MHC-B that are sequence differences independent of the presence of the insert.

Another interesting cluster of sequence divergence between MHC-A and MHC-B was found just carboxyl-terminal to the S1 head region of the molecule. This region maps to subfragment 2 (S2). In *Drosophila*, alternative splicing in this region results in MHC isoforms with different speeds of contraction (6). Throughout the rod region of the molecule there are also clusters of sequence divergence between MHC-A and MHC-B which may contribute to their tendency to form homodimers. Finally, as has been found for all MHC isoforms (32, 8), the extreme carboxyl terminus appears to be isoform specific. It has been shown that for nonmuscle myosins, the extreme carboxyl terminus participates in the formation of myosin filaments (16) and thereby may influence MHC-A and MHC-B homopolymer formation.

There are many similarities, but also important differences, in the distribution of myosin isoforms in *Xenopus* interphase and mitotic cells revealed by our experiments and those reported for human HeLa and melanoma cells by Maupin et al. (26). In *Xenopus*, the distribution of these nonmuscle myosin isoforms is more separate, which is intriguing. Nonmuscle myosin has previously been observed both in the cortex of cells and in stress fibers (9, 1, 38) and therefore the observation of myosin in these locations in *Xenopus* A6 and XTC cells is no surprise. However, the almost complete segregation of myosin isoforms, MHC-A in stress fibers and MHC-B at the cell periphery, coupled with their different enzymatic properties, is a new finding with interesting functional implications. MHC-A may function to maintain tension and could also be involved in the retrograde motion of stress fibers that has been observed in many cells (14). The presence of MHC-B in the cell cortex, especially its concentration in the lamellipodium of rapidly migrating cells, suggests a role for this myosin isoform in cell locomotion. Cell locomotion is known to involve morphological polarization, membrane extension, cell-substratum attachments, contractile force, and traction and finally release of attachments. However, exactly how the membrane extends and how the cell moves forward is unknown. There are at least two models to explain the protrusive force generation involved in lamellipodium extensions (for reviews see references 24, 28). One model is based on evidence suggesting that local actin polymerization in itself is an adequate energy source for extension against the mechanical resistance provided by the cell membrane. The second model involves motor protein-driven protrusive force generation. Myosin I, based on its intracellular location at the anterior of migrating amoebae (10, 3) and its localization to protrusive structures in migrating fibroblasts (7) could be one of the motor proteins responsible for leading edge extension and/or retraction. Myosin II has not previously been thought to be involved in protrusion because it was thought to be absent from such structures. However, recently Maupin et al. (26) immunolocalized some MHC-B in regions of membrane protrusions such as ruffling edges and nascent lamellipodia. Moreover, our report describes for the first time a high

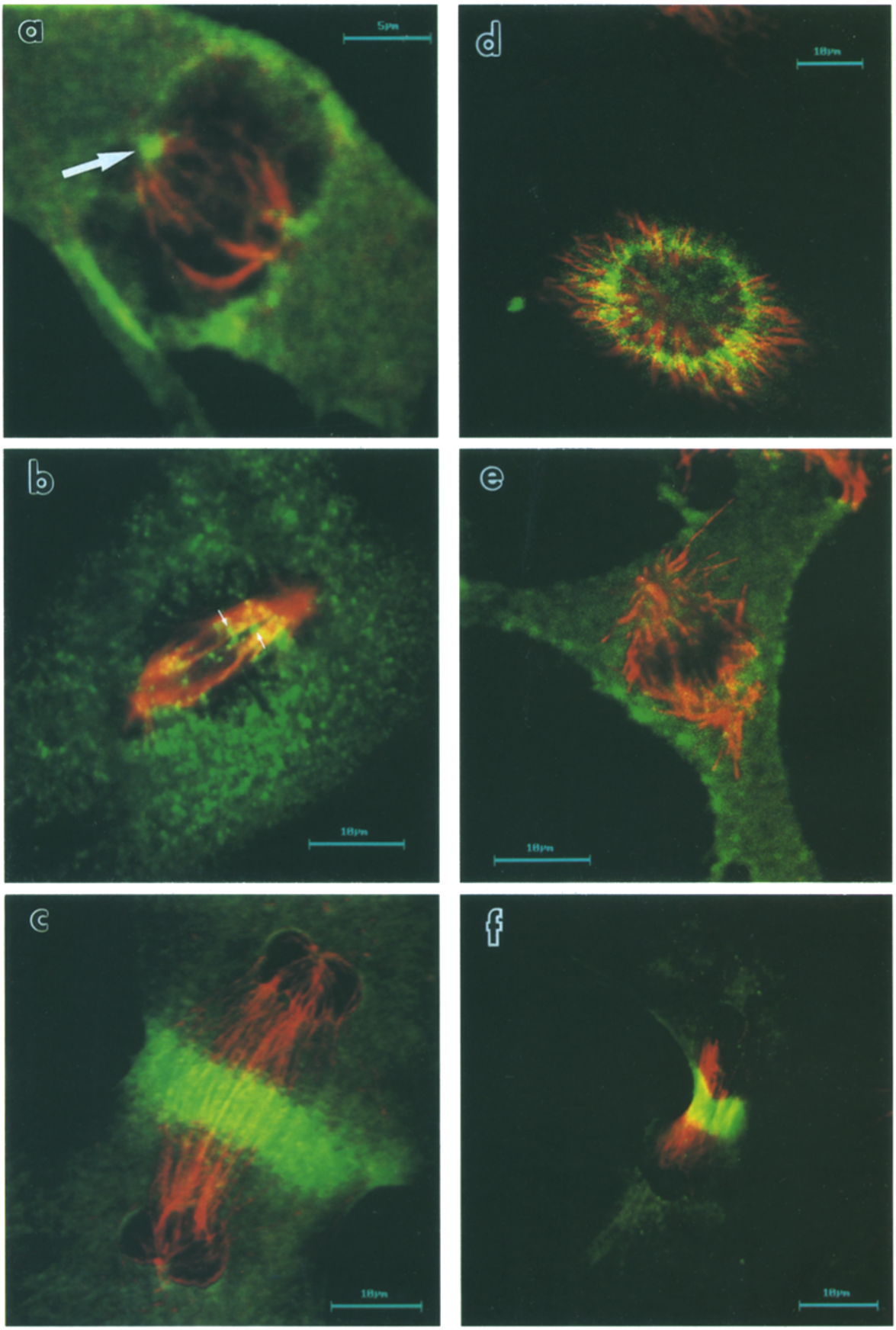
a
5μm
d
10μm
b
10μm
e
10μm
c
10μm
f
10μm

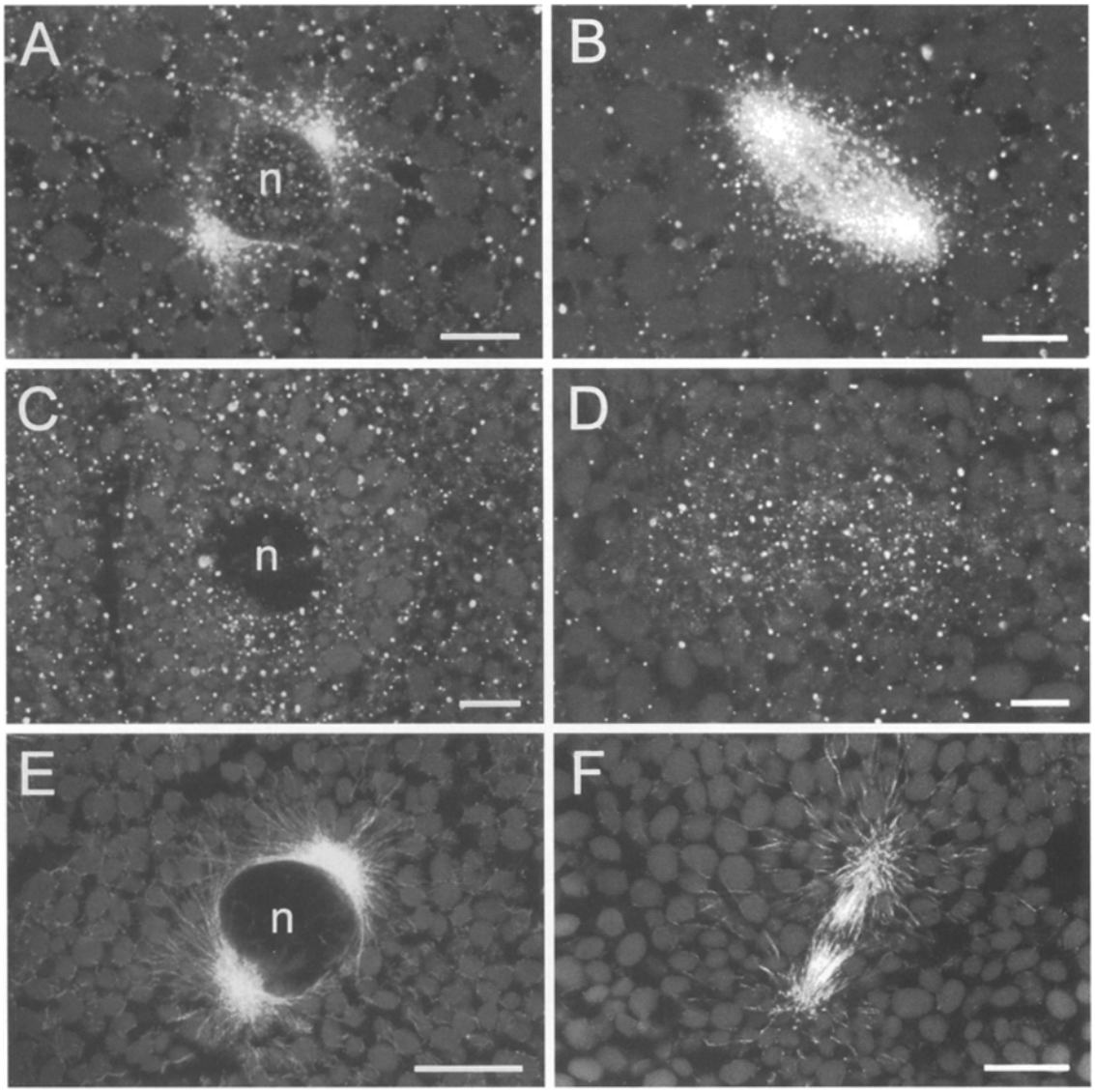

Figure 7. MHC-A localization in *Xenopus* blastomeres. Punctate MHC-A staining is associated with interphase microtubule arrays (*A*) and mitotic spindles in 8-h. blastomeres (*B*). Extraction of 6 h blastulae with microtubule stabilizing buffer (80 mM K Pipes, pH 6.8, 1 mM $MgCl_2$, 5 mM EGTA, 0.5 μM taxol, 0.5% TX-100) removes much of the microtubule and spindle associated MHC-A staining from interphase (*C*) and mitotic (*D*) blastomeres. Staining with DM1A anti-δ-tubulin reveals that interphase microtubules (*E*) and spindles (*F*) remain intact after extraction. MHC-A antiserum was diluted 1:100 in TBS (with 0.1% NP-40 and 1% BSA). The cell margins in all panels are outside of the margins of the micrographs. The gray bodies seen in the cytoplasm are yolk platelets. All scale bars are 10 μm.

concentration of a myosin II motor protein, namely MHC-B, in the lamellipodium of a highly polarized, rapidly migrating cell. These results suggest that the MHC-B motor could be part of the motile force underlying lamellipodial extension and/or retraction or in the contraction that pulls the cell body forward.

The different patterns of disruption of the two myosin isoforms, when cells are exposed to cytochalasin B, is consistent with their functional segregation and also suggests that F-actin is organized into (at least) two distinct populations in *Xenopus* cells. One population is responsible for the formation of stress fibers, colocalizes with MHC-A,

Figure 6. Subcellular localization of MHC-A and MHC-B in mitotic cells. *Xenopus* A6 cells at various stages of mitosis were fixed by method 2 and processed for confocal microscopy. *a–c*, MHC-A (*green*) and tubulin (*red*) staining during prophase (*a*), metaphase (*b*), and telophase (*c*). MHC-A localizes to the spindle poles (*arrow*) in prophase, and also has a diffuse cytoplasmic localization. Bright spots of MHC-A fluorescence (*arrows*) are present in the mitotic spindle apparatus during metaphase. MHC-A is concentrated in the contractile ring in telophase. (*d–f*) MHC-B (*green*) and tubulin (*red*) staining during prophase (*d*), metaphase (*e*), and telophase (*f*). MHC-B localizes to the nuclear envelope during prophase, has a diffuse cytoplasmic staining pattern during metaphase, and is confined to the contractile ring during telophase. Bars: (*a*) 5 μm; (*b–f*) 10 μm.

and depolymerizes on cytochalasin B treatment causing MHC-A to collapse to the perinuclear region. The other is composed of cortical actin, has MHC-B associated with it, and on treatment with cytochalasin B collapses to discrete foci that contain residual F-actin and MHC-B. Interestingly, these foci localize mainly to microtubule ends suggesting that microtubules play a role in cortical actin filament dynamics. Such a role could include provision of a stable scaffold on which the cortical actin filament network could be assembled, organized, and even disassembled. Protrusion at the leading edge of the cell during migration and growth involves continual assembly and disassembly of the cortical actin filament network which may thus require the presence of a more stable scaffold to assist in its organization.

The separate localization of MHC-A and MHC-B in mitotic cells also suggests different functions for these nonmuscle myosin isoforms in cell cycle progression. In prophase of mitosis, MHC-B is localized to the nuclear membrane suggesting that it may be involved in some aspect of nuclear envelope breakdown. The nuclear localization of this isoform in prophase is also interesting because previously we reported that this isoform of the nonmuscle myosin heavy chain, but not MHC-A, is phosphorylated by cdc2 kinase during meiosis in *Xenopus* oocytes (22). This would put MHC-B at the right place, during the right time, for this phosphorylation.

The observation that MHC-A is in the mitotic spindle is of note. Previous reports on the general distribution of myosin in mitosis were contradictory, some reporting myosin in the spindle while others did not (9, 1, 38). Here we have shown, using several different antibodies and three different cell types, that MHC-A, but not MHC-B, is localized to the mitotic apparatus. The role of MHC-A in the mitotic spindle remains unclear. However, its extraction with detergent-containing buffer suggests that it is associated with membrane vesicles and thus may not play a role in chromosome movement.

Determining the function of myosin isoforms in nonmuscle cells may help elucidate the mechanisms by which cells divide, move, and perform a variety of other motile activities. Our studies in *Xenopus* have allowed for a more extensive analysis of MHC-A and MHC-B compared to previous studies because of our ability to make correlations between enzymatic activity and localization.

The authors thank Dr. Donald Bottaro (National Cancer Institute, National Institutes of Health [NIH] for critical reading of the manuscript and Dr. Maryanne Conti (National Heart, Lung, and Blood Institute, NIH) for Xenopus MHC-A carboxyl-terminal sequence which allowed us to make Xenopus MHC-A–specific antibodies. We also thank Dr. Naina Bhatia-Dey for providing us with the full-length Xenopus MHC-A sequence so that a comparison of divergent amino acid regions could be made between Xenopus MHC-A and MHC-B.

Received for publication 29 March 1996 and in revised form 6 June 1996.

References

1. Aubin, J.E., W. Weber, and M. Osborn. 1979. Analysis of actin and microfilament associated proteins in the mitotic spindle and cleavage furrow of PtK2 cells by immunofluorescence. *Exp. Cell Res.* 124:93–109.
2. Baines, I.C., and E.D. Korn. 1994. *Acanthamoeba castellanii:* a model system for correlative biochemical and cell biological studies. *In* Cell Biology: A Laboratory Handbook. Academic Press, Aarhus, Denmark. J.E. Celis, editor. pp. 405–411.
3. Baines, I.C., A. Corigliano-Murphy, and E.D. Korn. 1995. Quantification and localization of phosphorylated myosin I isoforms in *Acanthamoeba castellanii. J. Cell Biol.* 130:591–603.
4. Bhatia-Dey, N., R.S. Adelstein, and I.B. Dawid. 1993. Cloning of the cDNA encoding a myosin heavy chain B isoform of *Xenopus* nonmuscle myosin with an insert in the head region. *Proc. Natl. Acad. Sci. USA.* 90: 2856–2859.
5. Cheng, T. P.O., N. Murakami, and M. Elzinga. 1992. Localization of myosin-IIB at the leading edge of growth cones from rat dorsal-root ganglionic cells. *FEBS Lett.* 311:91–94.
6. Collier, V.L., W.A. Kronert, P.T. O'Donnell, K.A. Edwards, and S.I. Bernstein. 1990. Alternative myosin hinge regions are utilized in a tissue-specific fashion that correlates with muscle contraction speed. *Genes Dev.* 6: 885–895.
7. Conrad, P.A., K.A. Giuliano, G. Fisher, K. Collins, P.T. Matsudaira, and D.L. Taylor. 1993. Relative distribution of actin, myosin I, and myosin II during the wound healing response of fibroblasts. *J. Cell Biol.* 120:1381–1391.
8. Feghali, R., and L.A. Leinwand. 1989. Molecular genetic characterization of a developmentally regulated human perinatal myosin heavy chain. *J. Cell Biol.* 108:1791–1797.
9. Fujiwara, K., and T.D. Pollard. 1976. Fluorescent antibody localization of myosin in the cytoplasm, cleavage furrow and mitotic spindle of human cells. *J. Cell Biol.* 71:848-875.
10. Fukui, Y., T.J. Lynch, H. Brzeska, and E.D. Korn. 1989. Myosin I is located at the leading edges of locomoting *Dictyostelium* amoeba. *Nature (Lond.).* 341:328–331.
11. Fukui, Y., A. De Lozanne, and J. A. Spudich. 1990. Structure and function of the cytoskeleton of a *Dictyostelium* myosin-defective mutant. *J. Cell Biol.* 110:367-378.
12. Gard, D.L. 1993. Confocal immunofluorescence microscopy of microtubules in amphibian oocytes and eggs. *Methods Cell Biol.* 38:241–264.
13. Gard, D.L., S. Hafezi, T. Zhang, and S.J. Doxsey. 1990. Centrosome duplication continues in cyclohexamide-treated *Xenopus* blastulae in the absence of a detectable cell cycle. *J. Cell Biol.* 110:2033–2042.
14. Giuliano, K.A., and D.L. Taylor. 1990. Formation, transport, contraction, and disassembly of stress fibers in fibroblasts. *Cell Motil. Cytoskeleton.* 16:14–21.
15. Hartshorne, D.J. 1987. Biochemistry of the contractile process in smooth muscle. *In* Physiology of the Gastrointestinal Tract. L.R. Johnson, editor. Raven Press, New York. pp. 423–482.
16. Hodge, T.P., R. Cross, and J. Kendrick-Jones. 1992. Role of the COOH-terminal nonhelical tailpiece in the assembly of a vertebrate nonmuscle myosin rod. *J. Cell Biol.* 118:1085–1095.
17. Katsuragawa, Y., M. Yanagisawa, A. Inoue, and T. Masaki. 1989. Two distinct nonmuscle myosin heavy chain mRNAs are differently expressed in various chicken tissues. *Eur. J. Biochem.* 184:611–616.
18. Kawamoto, S., and R.S. Adelstein. 1991 Chicken nonmuscle myosin heavy chains: differential expression of two mRNAs and evidence for two different polypeptides. *J. Cell Biol.* 112:915–924.
19. Kelley, C.A., and R.S. Adelstein. 1990. The 204-kDa smooth muscle myosin heavy chain is phosphorylated in intact cells by casein kinase II on a serine near the carboxyl-terminus. *J. Biol. Chem.* 265:17876–17882.
20. Kelley, C.A., J.R. Sellers, P.K. Goldsmith, and R.S. Adelstein. 1992. Smooth muscle myosin is composed of homodimeric heavy chains. *J. Biol. Chem.* 267:2127–2130.
21. Kelley, C.A., M. Takahashi, J.H. Yu, and R.S. Adelstein. 1993. An insert of seven amino acids confers functional differences between smooth muscle myosins from the intestines and vasculature. *J. Biol. Chem.* 268:12848–12854.
22. Kelley, C.A., F. Oberman, J.K. Yisraeli, and R.S. Adelstein. 1995. A *Xenopus* nonmuscle myosin heavy chain is phosphorylated by cyclin-p34^{cdc2} kinase during meiosis. *J. Biol. Chem.* 270:1395–1401.
23. Laemmli, U.K. 1970. Cleavage of structural proteins during the assembly of the head of bacteriophage T4. *Nature (Lond.).* 227:680–685.
24. Lauffenburger, D.A., and A.F. Horwitz. 1996. Cell migration: a physically integrated molecular process. *Cell.* 84:359–368.
25. Ludowyke, R.I., I. Peleg, M.A. Beaven, and R.S. Adelstein. 1989. Antigen-induced secretion of histamine and the phosphorylation of myosin by protein kinase C in rat basophilic leukemia cells. *J. Biol Chem.* 264:12492–12501.
26. Maupin, P., C.L. Phillips, R.S. Adelstein, and T.D. Pollard. 1994. Differential localization of myosin II isozymes in human cultured cells and blood cells. *J. Cell Sci.* 107:3077–3090.
27. Miller, M., E. Bower, P. Levitt, D. Li, and P.D. Chantler. 1992. Myosin II distribution in neurons is consistent with a role in growth cone motility but not synaptic vesicle mobilization. *Neuron.* 8:25–44.
28. Mitchison, T.J., and L.P. Cramer. 1996. Actin-based cell motility and cell locomotion. *Cell.* 84:371–379.
29. Murakami, N., and M. Elzinga. 1992. Immunohistochemical studies on the distribution of cellular myosin II isoforms in brain and aorta. *Cell Motil. Cytoskeleton.* 22:281–295.
30. Pasternak, C., J.A. Spudich, and E.L. Elson. 1989. Capping of surface receptors and concomitant cortical tension are generated by conventional myosin. *Nature (Lond.).* 341:549–551.

31. Pato, M.D., J.R. Sellers, Y.A. Preston, E.V. Harvey, and R.S. Adelstein. 1996. Baculovirus expression of chicken nonmuscle heavy meromyosin II-B. *J. Biol. Chem.* 271:2689–2695.
32. Periasamy, M., D.F. Wieczorek, and B. Nadal-Ginard. 1984. Characterization of a developmentally regulated perinatal myosin heavy-chain gene expressed in skeletal muscle. *J. Biol. Chem.* 259:13573–13578.
33. Pollard, T.D., and E.D. Korn. 1973. *Acanthamoeba* myosin. I. Isolation from *Acanthamoeba castellanii* of an enzyme similar to muscle myosin. *J. Biol. Chem.* 248:4682–4690.
34. Rayment, I., W.R. Rypnjewski, K. Schmidt-Base, R. Smith, D.R. Tomchick, M.M. Benning, D.A. Winkelmann, G. Wesenberg, and H.M. Holden. 1993. Three-dimensional structure of myosin subfragment-1: a molecular motor. *Science (Wash. DC).* 261:50–58.
35. Rochlin, M.W., K. Itoh, R.S. Adelstein, and P.C. Bridgman. 1995. Localization of myosin IIA and B isoforms in cultured neurons. *J. Cell Sci.* 108: 3661–3670.
36. Rovner, A.S., Y. Freyzon, and K.M. Trybus. 1995. Chimeric substitutions of the actin-binding loop activate dephosphorylated but not phosphorylated smooth muscle heavy meromyosin. *J. Biol. Chem.* 270:30260–30263.
37. Saez, C.G., J.C. Myers, T.B. Shows, and L.A. Leinwand. 1990. Human nonmuscle myosin heavy chain mRNA: generation of diversity through alternative polyadenylation. *Proc. Natl. Acad. Sci. USA.* 87 :1164–1168.
38. Sanger, J.M., B. Mittal, J.S. Dome, and J.W. Sanger. 1989. Analysis of cell division using fluorescently labeled actin and myosin in living PtK2 cells. *Cell Motil. Cytoskeleton.* 14:201–219.
39. Sellers, J.R., and H.V. Goodson. 1995. Motor Proteins 2: Myosins. *Protein Profile.* 2:1323–1423.
40. Sellers, J.R., H.V. Goodson, and F. Wang. 1996. A myosin family reunion. *J. Muscle Res. Cell Motil.* 17:7–22.
41. Shohet, R.V., M.A. Conti, S. Kawamoto, Y.A. Preston, D.A. Brill, and R.S. Adelstein. 1989. Cloning of the cDNA encoding the myosin heavy chain of a vertebrate cellular myosin. *Proc. Natl. Acad. Sci. USA.* 86:7726–7730.
42. Simons, M., M. Wang, O.W. McBride, S. Kawamoto, K. Yamakawa, D. Gdula, R.S. Adelstein, and L. Weir. 1991. Human nonmuscle myosin heavy chains are encoded by two genes located on different chromosomes. *Circ. Res.* 69:530–539.
43. Smith, J.C., and J.R. Tata. 1991. *Xenopus* cell lines. *Methods Cell Biol.* 36: 635–654.
44. Spudich, J.A. 1994. How molecular motors work. *Nature (Lond.).* 372:515–518.
45. Takahashi, M., S. Kawamoto, and R.S. Adelstein. 1992. Evidence for inserted sequences on the head region of nonmuscle myosin specific to the nervous system. *J. Biol. Chem.* 267:17864–17871.
46. Uyeda T.Q.P., K.M. Ruppel, and J.A Spudich. 1994. Enzymatic activities correlate with chimaeric substitutions at the actin-binding face of myosin. *Nature (Lond.).* 368:567–569.
47. Warrick, H.M., and J. A. Spudich. 1987. Myosin structure and function in cell motility. *Annu. Rev. Cell Biol.* 3:379–421.